

KINEMATIC LINKAGE BETWEEN THE BROAD AND NARROW LINE EMITTING GAS IN AGN

R. ZAMANOV¹, P. MARZIANI¹, J. W. SULENTIC², M. CALVANI¹, D. DULTZIN-HACYAN³, R. BACHEV²
submitted May 15, 2002; accepted July 11, 2002

ABSTRACT

We investigate the radial velocity difference between the [OIII] $\lambda\lambda 4959, 5007$ and $H\beta$ lines for a sample of ≈ 200 low redshift AGN. We identify seven objects showing an [OIII] $\lambda 5007$ blueshift relative to $H\beta$ with amplitude larger than 250 km s^{-1} (blue “outliers”). These line shifts are found in sources where the broad high ionization lines (e.g. CIV $\lambda 1549$) also show a large systematic blueshift. Such blueshifts occur only in the population A region of the Eigenvector 1 parameter domain (that also contains NLSy1 sources). We suggest that [OIII] $\lambda\lambda 4959, 5007$ blueshifts are also associated with the high ionization outflow originating in these sources. This is a direct kinematic linkage between narrow and broad line emitting gas.

Subject headings: quasars: emission lines – quasars: general – galaxies: active

1. INTRODUCTION

Forbidden [OIII] $\lambda\lambda 4959, 5007$ emission arises in the narrow line region (NLR) of Active Galactic Nuclei (AGN). This emission has now been partly resolved in the nearest AGN, where the geometry of the line emitting gas has been found to be far from spherically symmetric. This suggests that measures of integrated [OIII] $\lambda\lambda 4959, 5007$ emission may correlate with source orientation to the line of sight (Hes et al. 1993; Sulentic, Marziani & Dultzin-Hacyan 2000a, and references therein). Observations and theoretical models both (e.g., Steffen et al. 1997; Sulentic & Marziani 1999; Moiseev et al. 2001) suggest a complex interplay between (where applicable) shocks driven by radio ejection and the ionizing continuum from the nucleus.

At the same time it is generally believed that radial velocity measures of the narrow emission lines (e.g. narrow $H\beta$ and [OIII] $\lambda\lambda 4959, 5007$) provide a reliable measure of the systemic, or rest-frame, velocity. [OIII] $\lambda 5007$ is preferred because it is not superimposed on a much stronger broad line component. Limited HI, CO and absorption line measures of the host galaxy rest frame suggest that [OIII] $\lambda\lambda 4959, 5007$ usually gives consistent results within 200 km s^{-1} (de Robertis 1985; Whittle 1985; Wilson & Heckman 1985; Condon et al. 1985; Stirpe 1990; Alloin et al. 1992; Evans et al. 2001). Several observations, however, indicate that the Narrow Line Seyfert 1 (NLSy1) prototype I Zw 1 shows an [OIII] $\lambda\lambda 4959, 5007$ blueshift of $\Delta v_r = -500 \text{ km s}^{-1}$ relative to other rest frame measures (Boroson & Oke 1987). This corresponds to a 10 \AA shift which is larger than any conceivable measurement or calibration errors; see Marziani et al. 1996).

We report here a study of the velocity shift of [OIII] $\lambda 5007$ relative to $H\beta$. Our aim was to identify objects with large radial velocity disagreement between [OIII] $\lambda 5007$ and $H\beta$ and their relationship with the general population of AGN.

2. SAMPLE AND DATA ANALYSIS

We measured the (narrow line) velocity difference between the peak of [OIII] $\lambda 5007$ and of $H\beta$ using our database of spectra for $n = 216$ AGN. The dataset includes CCD spectra obtained over the past ≈ 10 years for studies of the $H\beta$ region in

Seyfert 1 and low redshift ($z \lesssim 0.8$) quasars. Spectra were obtained with the following telescopes and spectrographs: ESO 1.5m (B&Ch), San Pedro Martir 2.2m (B&Ch), Calar Alto 2.2m (B&Ch), KPNO 2.2m (Gold), and Asiago 1.82m (B&Ch). Results based on these spectra can be found in Marziani et al. (1996) and Sulentic et al. (2000a, 2002). The unpublished part of this dataset will appear in a forthcoming paper (Marziani et al. 2002). Spectra were taken with very similar instrumental setups yielding resolution in the range $4\text{--}7 \text{ \AA}$ FWHM. The S/N of our spectra is typically in the range $\approx 20\text{--}40$ (minimum 12). The high S/N and the moderate resolution make this sample appropriate for the study of line shifts because FWHM and shift measures are not significantly affected by undersampling. Our AGN sample has an average source absolute B magnitude $\langle M_B \rangle \approx -23.7 \pm 2.0$ ($H_0 = 50 \text{ km s}^{-1} \text{ Mpc}^{-1}$, $q_0 = 0$).

We de-redshifted the spectra using an initial $H\beta$ measurement for v_r in all sources where an $H\beta$ narrow component could be identified. Optical FeII_{opt} emission blends were then subtracted using the template method (Boroson & Green 1992). At this point, we measured v_r for $H\beta$ a second time, as well as v_r for [OIII] $\lambda 5007$. Hereafter we will consider only the difference in radial velocities $\Delta v_r = v_r([\text{OIII}]\lambda 5007) - v_r(H\beta)$ measured from the FeII_{opt} subtracted spectra. The measurement of Δv_r turned out to be possible for 187 sources. The 23 excluded sources include 7 with no detectable [OIII] $\lambda\lambda 4959, 5007$ emission and 16 with a very poorly defined $H\beta$ line peak.

3. RESULTS

3.1. [OIII] $\lambda\lambda 4959, 5007$ Line Shift Distribution

The distribution of Δv_r measures is shown in Fig. 1a. The values range from -950 to $+280 \text{ km s}^{-1}$ with an average $\langle \Delta v_r \rangle = -30 \text{ km s}^{-1}$. The sample standard deviation is $\pm 135 \text{ km s}^{-1}$. The median value is $\overline{\Delta v_r} = -7 \text{ km s}^{-1}$. 50% of the measurements fall in the interval from -49 to $+16 \text{ km s}^{-1}$, so we adopt the first and third quartile as confidence limits, $\overline{\Delta v_r} = -7_{-42}^{+23} \text{ km s}^{-1}$. The central bins of our Δv_r distribution are dominated by measurement errors, with typical values estimated to be in the range $40\text{--}50 \text{ km s}^{-1}$ at 1σ confidence level. The continuous distribution of measures in the

¹ INAF, Osservatorio Astronomico di Padova, Vicolo dell’Osservatorio 5, I-35122 Padova, Italy

² Department of Physics and Astronomy, University of Alabama, Tuscaloosa, AL 35487, USA

³ Instituto de Astronomía, UNAM, Apdo. Postal 70-264, 04510 Mexico D.F., Mexico

⁴ Based in part on data collected at ESO La Silla.

range $-200 \text{ km s}^{-1} \lesssim \Delta v_r \lesssim +200 \text{ km s}^{-1}$ suggests that the $[\text{OIII}]\lambda 5007$ redshift measurements are consistent with $\text{H}\beta$ to within the above range in more than 90% of the sources. The distribution of shifts is not symmetric around $v_r = 0 \text{ km s}^{-1}$ but is skewed toward the blue. Shifts in the range $-200 \lesssim \Delta v_r \lesssim -100$ are three times more frequent than redshifts in the range $100 \lesssim \Delta v_r \lesssim 200 \text{ km s}^{-1}$. The maximum shift to the red $\Delta v_r \approx 280 \text{ km s}^{-1}$ while shifts up to $\Delta v_r \approx -1000 \text{ km s}^{-1}$ are observed on the blue side. The shift distribution reveals seven sources with $[\text{OIII}]\lambda\lambda 4959, 5007$ shift ($\Delta v_r \lesssim -250 \text{ km s}^{-1}$), which are listed in Table 1.

The relatively rare outliers, (referred to hereafter as “blue outliers”), are not randomly distributed in an Eigenvector 1 (=E1) (Sulentic et al. 2000; §3.3) space representation of AGN diversity. Figure 1b plots $[\text{OIII}]\lambda 5007$ shift amplitude Δv_r versus full-width half maximum of the $\text{H}\beta$ broad component $[\text{FWHM}(\text{H}\beta_{\text{BC}})]$, and Fig. 1c identifies the blue outlier sources in the E1 optical plane. Fig. 1b and Fig. 1c suggest that large $[\text{OIII}]\lambda 5007$ blueshifts ($\Delta v_r \lesssim -300 \text{ km s}^{-1}$) are confined to sources with $\text{FWHM}(\text{H}\beta_{\text{BC}}) \lesssim 4000 \text{ km s}^{-1}$. The largest negative values ($\Delta v_r \lesssim -600 \text{ km s}^{-1}$) is found at $\text{FWHM}(\text{H}\beta_{\text{BC}}) \lesssim 2000 \text{ km s}^{-1}$. One radio-loud outlier PKS 0736 (-433 km s^{-1} blueshift) is found. It shows the largest $\text{FWHM}(\text{H}\beta_{\text{BC}})$ for any of the seven identified extreme blue outliers. Figure 2 presents FeII subtracted spectra of the region of $\text{H}\beta$ and $[\text{OIII}]\lambda\lambda 4959, 5007$ region for the 7 blue outlier sources. They also show preferentially blue Balmer line asymmetries as was previously noted for NLSy1 sources.

3.2. Are the Outliers Real ?

Even though the $[\text{OIII}]\lambda\lambda 4959, 5007$ emission in these sources is weak, it is difficult to doubt the detection of such large displacements in both $[\text{O III}]\lambda 4959$ and $[\text{O III}]\lambda 5007$ relative to the reference frame defined by $\text{H}\beta$ (Figure 2). We are able to measure the radial velocity of both $[\text{OIII}]\lambda 5007$ and $[\text{O III}]\lambda 4959$ including those with low equivalent width. The velocities are always consistent within 100 km s^{-1} and the equivalent width ratio of $[\text{OIII}]\lambda 5007$ and $[\text{O III}]\lambda 4959$ is about 3:1 for the blue outliers, as expected (see Table 1). This and the fact that the shifts as well as the equivalent widths are different from sources to source, indicates that the $[\text{OIII}]\lambda\lambda 4959, 5007$ lines, although weak, are not strongly affected by the FeII_{opt} subtraction. We further checked with subtraction of a theoretical template in the region $4800 - 5100 \text{ \AA}$ (Sigut & Pradhan, 2002), and the results, shown in Fig. 2, are very similar.

One of the seven blue outliers (I Zw1) has reliable independent host galaxy redshift determinations based on HI 21 cm and molecular CO observations (see e.g., Schöniger & Sofue 1994). This is likely to be an accurate and reliable rest frame determination for at least three reasons: 1) the HI and CO lines profiles match very closely in shape, width and centroid velocity, 2) the profiles are symmetric and 3) the profiles are steep sided double horns. The centroid measures are consistent with the velocity of the peak of the $\text{H}\beta$ emission line profile and not with $[\text{OIII}]$.

Sources with $\text{FWHM}(\text{H}\beta_{\text{BC}}) \lesssim 4000 \text{ km s}^{-1}$ show a sharply peaked, Lorentzian $\text{H}\beta$ profile. In such cases the narrow line component is uncertain because no profile inflection is seen. Even if the $\text{H}\beta$ profile is completely ascribed to the broad component, it seems that the $\text{H}\beta$ peak is nonetheless a good estimator of the quasar systemic velocity (this result is expected if the line comes from an extended accretion disk). We might expect to detect a *blueshifted* $\text{H}\beta_{\text{NC}}$ analog to the $[\text{OIII}]$ lines, but

given the low equivalent width $W([\text{OIII}]\lambda 5007)$ we normally expect $W([\text{OIII}]\lambda 5007)/W(\text{H}\beta_{\text{NC}}) \sim 10$, such a blueshifted component will be lost in the noise.

We also attempted to identify red outliers (there are seven objects with $\Delta v_r \gtrsim 150 \text{ km s}^{-1}$ which form an extended red tail in the shift distribution). In all cases, we find that the top of $\text{H}\beta$ is complex or even multi-peaked. This means that the use of $\text{H}\beta$ as a reference is sometimes ambiguous. Independent rest frame measures for two of these sources are consistent with an $[\text{OIII}]$ derived radial velocity. We therefore interpret Figure 1a as consistent with three populations: 1) A scatter population associated in part with measurement errors; 2) a real, but relatively rare population of sources where $[\text{OIII}]\lambda 5007$ shows an intrinsic large blue shift relative to the local rest frame (the blue outliers); 3) an intermediate population, in the range $-250 \text{ km s}^{-1} \lesssim \Delta v_r \lesssim -100 \text{ km s}^{-1}$, probably containing both sources with intrinsic blue shifts and sources with larger $\text{H}\beta$ v_r uncertainty.

The preferred location of the blue outliers in E1 motivated us to search for corroboration among samples of phenomenologically similar (see next section) sources. Grupe, Thomas & Leighly (2001) identify a blueshift of 570 km s^{-1} in RXJ2217-59. Our quick look of other (FeII corrected) spectra (Grupe et al. 1999) revealed at least three other sources with obvious blueshifts in the range -300 to -500 km s^{-1} (RXJ1036-35, RXJ 2340-53 and MS2340-15).

3.3. Blue outliers and Eigenvector 1

Further insight and confidence about the reality of blue outliers can be gained from considering the distribution in the Eigenvector 1 diagrams (Sulentic et al. 2000b). The principal physical driver of E1 is assumed to be the luminosity-to-mass ratio (\propto accretion rate) convolved with source orientation (Marziani et al. 2001) and/or the black hole mass (Boroson 2002; Zamanov & Marziani 2002). The distribution of blue outliers in the E1 optical plane Fig. 1c) is obviously different from that of the general AGN population. The blue outliers occupy the lower right part of the diagram and are exclusively population A/NLSy1 ($\text{FWHM}(\text{H}\beta_{\text{BC}}) \lesssim 4000 \text{ km s}^{-1}$) sources. A 2D Kolmogorov-Smirnov (see e.g. Fasano & Franceschini, 1987) suggests that the parameter space occupation of the *blue* outliers is significantly different than the majority of AGN at a confidence level of 0.990–0.999. The preferred location of the blue outliers in E1 motivated us to search for other $[\text{OIII}]$ blueshifts among samples of phenomenologically similar sources. Grupe, Thomas & Leighly (2001) identify a blueshift of 570 km s^{-1} in RXJ2217-59. Our quick look of other (FeII corrected) spectra (Grupe et al. 1999) revealed at least three other sources with obvious blueshifts in the range -300 to -500 km s^{-1} (RXJ1036-35, RXJ 2340-53 and MS2340-15).

Figure 3 in Sulentic et al (2000a) involving $\text{CIV}\lambda 1549$ centroid shift vs. $\text{FWHM H}\beta$ shows a striking similarity to Figure 1b of this paper. There is a HIL blueshift in the same AGN (population A) where we find all of the blue outliers. The simplest interpretation is that we are seeing a kinematic linkage between BLR and NLR HIL. A source by source comparison reveals 5 of 7 blue outliers with HST FOS archival spectra of the $\text{CIV}\lambda 1549$ line. The blue outliers show CIV blueshifts (at $\text{FWHM}(\text{CIV}\lambda 1549)$) between $V = -503$ and -1936 km s^{-1} . This motivates us to look at all sources in our full sample with CIV shift ($>600 \text{ km/s}$) and $W([\text{OIII}]) (<15\text{\AA})$, properties similar to the blue outliers. We find 12 additional sources where: 1) no narrow $\text{H}\beta$ peak and/or $[\text{OIII}]$ line is observed (sometimes

simply due to noisier than average spectra), 2) smaller, likely significant, [OIII] blueshifts are observed (e.g. -200 km/s for PG1444+407) and 3) a peak+blue wing structure is observed. In the numerous latter cases we see a narrow unshifted [OIII] line with a strong blue wing. In the absence of the peak we would measure a blueshift in the blue outlier velocity range. This motivates us to propose that the blue outliers represent sources where the classical extended NLR is absent or suppressed. The peak+ blue wing cases represent sources where both the (usually strong) classical and the (usually weak) blue shifted NLR components are present. The concept of two distinct NLR components is reinforced by sources like NGC7213 (Busko & Steiner 1988) and RXJ0148-27 (Grupe et al. 1999) where the unshifted and the blueshifted [OIII] components are actually resolved.

4. THE EXTREME OF AN EXTREME: LARGE SHIFTS GOVERNED BY ORIENTATION?

An obvious question involves whether or not the [OIII] λ 5007 blue outliers are peculiar AGN – a new, previously unknown AGN class. They do not appear to be part of a continuous distribution of [OIII] λ 5007 velocity shifts. However, even if the distribution of [OIII] λ 5007 outliers is not consistent with the other AGN in the E1 parameter plane, blue outliers lie near an extremum in the AGN occupied domain rather than outside of it. If we consider our tentative grid of expected L/M and i values in the E1 plane (Marziani et al. 2001), we see that the blue outliers may be the product of special circumstances: 1) a large L/M ratio, and 2) a small inclination ($i \rightarrow 0^\circ$). Of course these two circumstances do not explain the absence of the classical NLR. One possibility is 3) that these sources are young quasars (see below). It has been suggested that radio-quiet NLSy1 are the equivalent of BL Lacs. We infer that our blue outliers (the ones observed almost face-on, with largest CIV λ 1549 and [OIII] λ 5007 blueshifts) may be the radio-quiet analogous of BL Lac. We note that the single RL blue outlier identified PKS0736+01 involves an optically violently variable (OVV) quasar.

We constructed a purely kinematical model in which [OIII] λ 4959,5007 and CIV λ 1549 are both assumed to arise in a radial flow constrained in a cone of half-opening angle $\Theta_0 \approx 85^\circ$ (e.g. a high ionization, optically thin wind) where the receding part of the flow is obscured by an optically thick accretion disk (i.e., we are able to see the approaching part of the flow and the near side of the disk which is assumed to emit H β). We assumed that radial motions in the gas were a fixed fraction (1.5) of the local virial velocity. We integrated over a region $100 R_g \leq r \leq 10^5 R_g$ for CIV λ 1549 and over a region $300 R_g \leq r \leq 10^5 R_g$ for [OIII] λ 5007, with emissivity power law-indices $q = -2$ (CIV λ 1549) and $q = -1$ ([OIII] λ 5007). Fig. 3 shows the resulting model profiles for a viewing angle $i \approx 15^\circ$. The width and shift of both lines are accounted for. We suggest, without considering this particular model as a physi-

cal one, that emission from outflowing gas, possibly associated to a disk wind, can explain the observed profiles. The occurrence of large [OIII] λ 5007 shifts seems to be associated with low $W([OIII]\lambda 5007)$. Our model integration also consistently suggests a *very compact* NLR ($r \sim 1$ pc for a black hole mass 10^8 solar masses). In this case, the receding part of the outflow may be more easily hidden by an optically thick disk extending to ~ 1 pc (this is a requirement also to avoid double peaked profiles). The filling factor needed to explain the [OIII] λ 5007 luminosity of I Zw 1 and PG 1543+489 can be reasonably small, $\sim 10^{-3}$. It is intriguing that a compact NLR complements several lines of evidence suggesting that NLSy1s are young AGN. Large $W([OIII]\lambda 5007)$ would imply a larger emitting volume and hence may be associated with lower [OIII] λ 5007 shifts. The frequent observations of blueward asymmetry close to the [OIII] λ 4959,5007 line profile base indicates that the same outflow may also be occurring in the innermost NLR of AGN with larger $W([OIII]\lambda 5007)$.

It is also interesting to note that Broad Absorption Line QSOs (BAL QSOs) are found more frequently in samples with low $W([OIII]\lambda 4959,5007)$ (Boroson & Meyers 1992; Turnshek et al. 1997). We do not find any BAL QSO among the outliers. In addition, the known low- z BAL QSO in our sample (PG 1004+13, PG 2112+059) with measurable [OIII] λ 5007 (2 out of 5) show shifts $\Delta v_r \sim 0$ km s $^{-1}$. This is also consistent with orientation playing a role and with blue outliers being oriented predominantly “face-on.” On the contrary, the CIV λ 1549 absorption/emission profiles of BAL QSOs suggest that they may be observed far from pole-on (Marziani et al. 2002, in preparation).

5. CONCLUSION

We find that the H β and [OIII] λ 5007 lines provide measures of the radial velocity of AGN usually consistent within ± 200 km s $^{-1}$. We identified infrequent ($\approx 5\%$ in a sample of 200 sources) AGN showing $\Delta v_r \lesssim -250$ km s $^{-1}$. They belong to the extreme population A sources that also show a large broad line CIV λ 1549 blueshift. This kinematic coupling of the NLR and BLR HIL emission most likely involves a wind or outflow. Our analysis suggests that blue outliers are not peculiar objects, but rather AGN viewed of extreme L/M with a compact NLR. A predominance of blueshifts in the sample indicates that [OIII] λ 5007 peak velocity is affected by outflow motions occurring in the innermost NLR.

We are very grateful to Giovanna Stirpe for fruitful discussions. The authors acknowledge support from the Italian Ministry of University and Scientific and Technological Research (MURST) through grant and Cofin 00–02–004. This research has made use of the NASA/IPAC Extragalactic Database (NED) which is operated by the JPL, Caltech under contract with the NASA.

REFERENCES

- Alloin, D., Barvainis, R., Gordon, M. A., & Antonucci, R. R. J. 1992, A&A, 265, 429.
 Boroson T., 2002, ApJ 565, 78
 Boroson T.A., Green R.F., 1992, ApJS, 80, 109
 Boroson T.A., & Meyers, K. A., 1992, ApJ, 397, 442
 Boroson, T. A. & Oke, J. B. 1987, PASP, 99, 809.
 Busko, I. & Steiner, J. 1988, MNRAS, 232, 525.
 Condon, J.J., Hutchings, J.B., & Gower, A.C. 1985, AJ, 90, 1642.
 de Robertis, M. 1985, ApJ, 289, 67.
 Evans, A. S., Frayer, D. T., Surace, J. A., & Sanders, D. B. 2001, AJ, 121, 1893.
 Hes, R., Barthel, P. D., & Fosbury, R. A. E. 1993, Nature, 362, 326
 Fasano G., & Franceschini A., 1987, MNRAS 225, 155
 Grupe, D., Beuermann, K., Mannheim, K., Thomas, H.-C., 1999, A&A, 350, 805
 Grupe, D., Thomas, H.-C., Leighly, K. M., 2001 A&A, 369, 450

Marziani, P., Sulentic, J. W., Dultzin-Hacyan, D., Calvani, M., Moles, M., 1996, *ApJS*, 104, 37
 Marziani, P., Sulentic, J.W., Zwitter, T., Dultzin-Hacyan, D., Calvani, M., 2001, *ApJ*, 558, 553
 Mirabel I.F., 1992, in *Relationships Between Active Galactic Nuclei and Starburst Galaxies*, ed. A. Filippenko, ASP Conf.Ser. vol. 31, p. 347
 Moiseev, A. V., Afanasiev, V. L., Dodonov, S. N., Mustsevoi, V. V., & Khrapov, S. S. 2001, *IAU Colloq. 184: AGN Surveys*, E79
 Richter, P., Savage, B.D., Wakker, B. P., Sembach, K. R., Kalberla, P. M. W., 2001, *ApJ*, 549, 281
 Schöninger, F., & Sofue, Y. 1994, *Å*, 283, 21
 Sigut T.A.A., Pradhan A.K., 2002, *ApJS*, in press (astro-ph/0206096)

Steffen, W., Gomez, J. L., Raga, A. C., & Williams, R. J. R. 1997, *ApJ*, 491, L73
 Stirpe, G. M. 1990, *A&AS*, 85, 1049.
 Sulentic, J. W. & Marziani, P. 1999, *ApJ*, 518, L9
 Sulentic J.W., Marziani P., & Dultzin-Hacyan D., 2000a, *AR A&A*, 38, 521
 Sulentic, J. W., Zwitter, T., Marziani, P., & Dultzin-Hacyan, D. 2000b, *ApJ*, 536, L5.
 Sulentic, J. W., Marziani, P., Zamanov, R., Bachev, R., Calvani, M. & Dultzin-Hacyan, D. 2002, *ApJ*, 566, L71
 Whittle, M. 1985, *MNRAS*, 213, 33.
 Wilson, A. S. & Heckman, T. M. 1985, *Astrophysics of Active Galaxies and Quasi-Stellar Objects*, Mill Valley, CA, University Science Books, 1985, 39
 Zamanov, R., & Marziani, P., 2002, *ApJ*, 571, L77

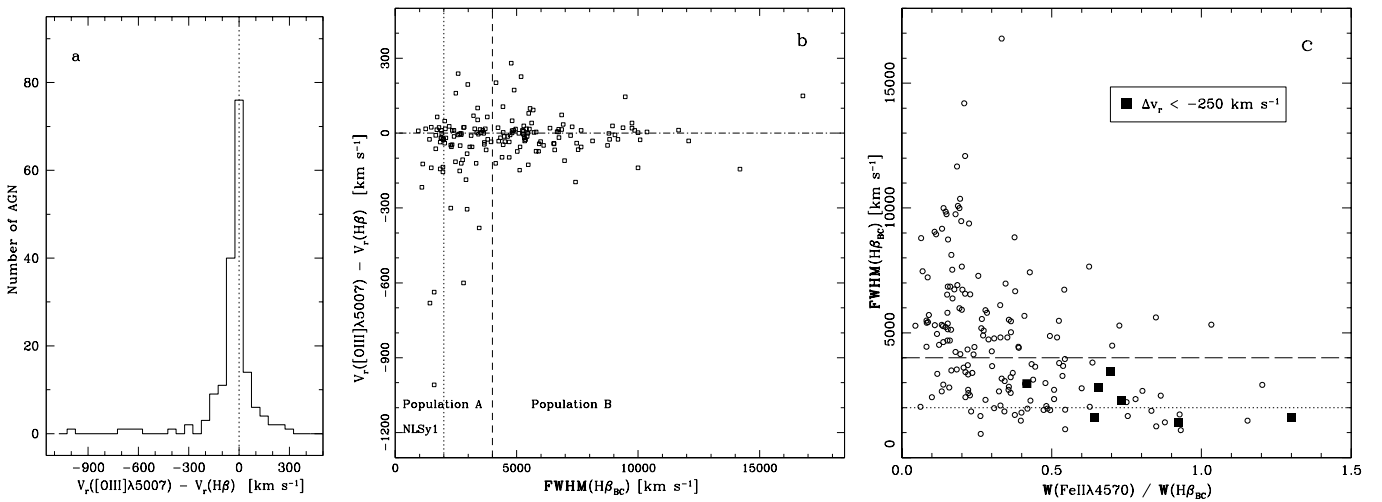


FIG. 1.— (a) Histogram showing the distribution of the radial velocity difference between the $[OIII]\lambda 5007$ and the $H\beta$ line. (b) The difference of the radial velocity between the $[OIII]\lambda 5007$ and $H\beta$ versus $\text{FWHM}(H\beta_{BC})$. The vertical dotted line marks the boundary of the NLSy1 galaxies. The vertical dashed line separates Population A and B sources. Seven objects with $\Delta v_r < -250 \text{ km s}^{-1}$ are visible. (c) Location of outliers in the $\text{FWHM}(H\beta_{BC})$ vs. R_{FeII} diagram (the optical Eigenvector-1 diagram). Filled squares represent the “blue outliers” ($\Delta v_r < -250 \text{ km s}^{-1}$).

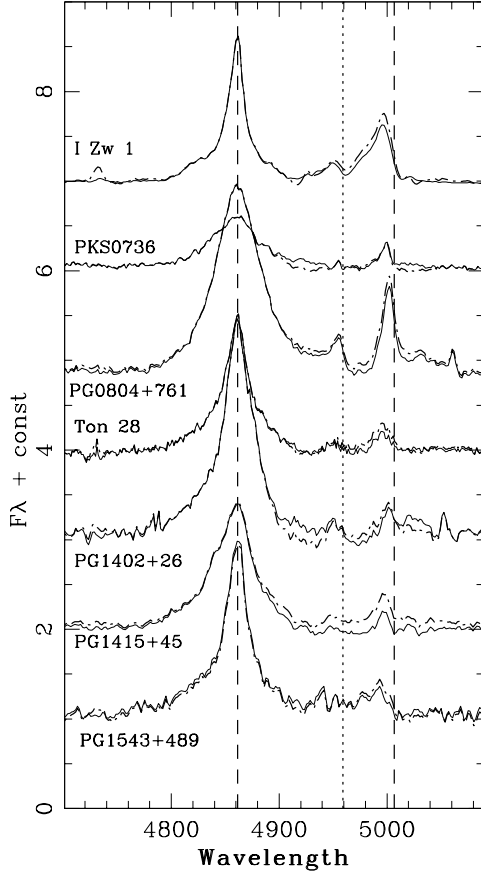


FIG. 2.— $H\beta$ spectral region of the “blue” outliers after the deredshift and subtraction of the FeII template. The spectra are normalized with respect to the local continuum and arbitrary constant added. The solid line corresponds to the subtraction of a I Zw 1-based empirical template, the dot-dashed line to the subtraction of a theoretical template. The vertical lines indicate the position of $H\beta$, [OIII] λ 4959 and [OIII] λ 5007. The difference in the radial velocities between the [OIII] λ 5007 lines and $H\beta$ is well visible.

TABLE 1

OBJECTS WITH ANOMALOUS DIFFERENCE OF THE RADIAL VELOCITIES BETWEEN THE [OIII] λ 5007 AND $H\beta$ (“BLUE OUTLIERS”).

Name	$z(H\beta)$	Δv_r	$W[\text{OIII}]\lambda 4959$	$W[\text{OIII}]\lambda 5007$	R_{FeII}	$\text{FWHM}(H\beta_{\text{BC}})$	$\Delta v_r(\text{CIV}\lambda 1549_{\text{BC}})$
		[km s^{-1}]	[\AA]	[\AA]		[km s^{-1}]	[km s^{-1}]
I Zw 1	0.0606	-640 ± 30	4.3	15.3	1.30	1600	-820
PKS 0736+01	0.1909	-430 ± 60	0.6	2.6	0.70	3460	... ^a
PG 0804+761	0.1014	-305 ± 30	3.3	10.1	0.42	2960	... ^a
Ton 28	0.3297	-680 ± 50	1.6	3.4	0.71	1860	-1120
PG 1402+261	0.1651	-300 ± 50	1.4	2.6	0.73	2280	-650
PG 1415+452	0.1151	-600 ± 50	1.1	2.9	0.66	2810	-950
PG 1543+489	0.4009	-950 ± 50	2.3	6.5	0.64	1600	-2630

^a HST/FOS observations not available.

Note. — The typical errors are $\pm 30\%$ in $W[\lambda 4959]$, $\pm 10\%$ in $W[\lambda 5007]$, ± 0.15 in R_{FeII} , $\pm 150 \text{ km s}^{-1}$ in $\text{FWHM}(H\beta)$, and $\pm 200 \text{ km s}^{-1}$ in $\Delta v_r(\text{CIV}\lambda 1549_{\text{BC}})$.

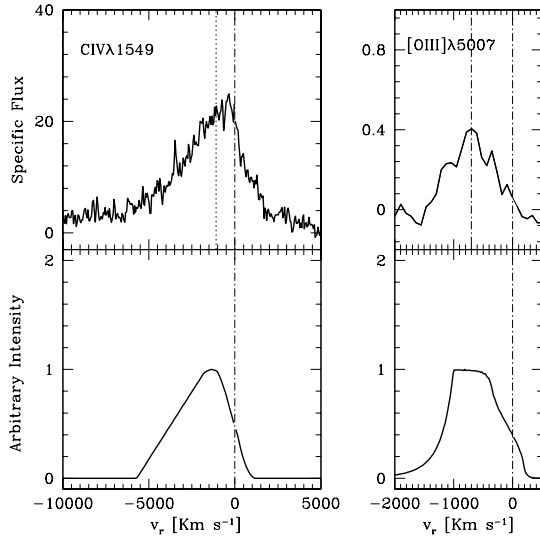


FIG. 3.— Upper panel: the $\text{CIV}\lambda 1549$ and $[\text{OIII}]\lambda 5007$ profile of Ton 28, a blue outlier. Lower Panel: $\text{CIV}\lambda 1549$ and $[\text{OIII}]\lambda 5007$ outflow model profiles, for optically thin gas moving at approximately the local escape velocity. Profiles have been computed for a cone of half-opening angle 85° , with the line of sight oriented at 15° with respect to the cone axis. The receding part of the flow is assumed to be fully obscured from the observer.